

SLL 80 291/P
copy 1

MDRL 78-13

Atmospheric Propagation of Partially Coherent Radiation

J.C. Leader

19980309 382

MCDONNELL DOUGLAS RESEARCH LABORATORIES

DTIC QUALITY INSPECTED 
MCDONNELL DOUGLAS

PLEASE RETURN TO:

BMD TECHNICAL INFORMATION CENTER
BALLISTIC MISSILE DEFENSE ORGANIZATION
7100 DEFENSE PENTAGON
WASHINGTON D.C. 20301-7100

U3876

MDRL 78-13

Atmospheric Propagation of Partially Coherent Radiation

J.C. Leader

J. Opt Soc. Am. 68, 175 (1978)

MCDONNELL DOUGLAS RESEARCH LABORATORIES

Box 516, Saint Louis, Missouri 63166 (314) 232-0232

MCDONNELL DOUGLAS



CORPORATION

Accession Number: 3876

Publication Date: Feb 01, 1978

Title: Atmospheric Propagation of Partially Coherent Radiation

Personal Author: Leader, J.C.

Corporate Author Or Publisher: McDonnell Douglas Research Laboratories, St. Louis, MO 63166 Report Number: MDRL 78-13
Report Number Assigned by Contract Monitor: SLL 80 291/P

Comments on Document: Archive, RRI, DEW

Descriptors, Keywords: Atmospheric Propagation Partial Coherent Radiation Rayleigh-Sommerfeld Integral Mutual Source
Atmosphere Angular Distribution Fourier Transform Amplitude Refractive Index

Pages: 00010

Cataloged Date: Nov 23, 1992

Document Type: HC

Number of Copies In Library: 000001

Record ID: 25181

Source of Document: DEW

Atmospheric propagation of partially coherent radiation*

J. Carl Leader

McDonnell Douglas Research Laboratories, McDonnell Douglas Corporation, St. Louis, Missouri 63166

(Received 17 August 1977)

An extended, Rayleigh-Sommerfeld integral method is used to derive expressions for the mutual coherence function and radiation intensity derived from a planar, partially coherent source propagating through the atmosphere. The derived results reduce to previous results for (i) coherent radiation propagation in the atmosphere and (ii) the relations relating the far-field intensity angular distribution and the source coherence for a partially coherent source *in vacuo*. A mathematical description of the predicted results in terms of the vacuum distribution and scattering functions (related to the Fourier-transformed two-source mutual coherence function) is permitted by this development. Analytical results are calculated for a homogeneous atmosphere and a source coherence that simulates a laser-illuminated rough surface. The effective far-field range is determined by the source size, wavelength, and source coherence length. The phase of the calculated mutual coherence function is determined by the field-point separation for off-axial propagation directions. Numerical results for the amplitude and phase coherence lengths are calculated and illustrated as a function of the source size, source coherence length, propagation angle, range, and refractive-index structure constant.

INTRODUCTION

Numerous investigators have studied the coherence of radiation propagating in the turbulent atmosphere using a variety of approaches including difference equations,¹ transport methods,² the Markov approximation,³ ladder ap-

proximations of the Bethe-Salpeter equation,⁴ and the Huygens-Fresnel principle.⁵ Beran⁶ has provided an excellent account of the consensus of these various approaches. All of the aforementioned studies, however, have been principally concerned with the propagation of initially coherent radiation because of its relevance to laser-propagation phenomena. Lee

*et al.*⁷ have examined the propagation of perfectly incoherent radiation in a turbulent medium, using the extended Huygens-Fresnel principle, to determine atmospheric effects on speckle phenomena. None of the previous studies have treated in detail the problem of atmospheric propagation of radiation derived from a partially (spatially) coherent source. The purpose of this paper is to examine the general case of partially coherent radiation propagation in a random medium.

The approach used in this study is essentially an extended Rayleigh-Sommerfeld integral method. This technique is analogous to the extended Huygens-Fresnel method⁸; however, it facilitates the analysis of the behavior of radiation coherence as a function of the propagation angle. Techniques previously employed to study coherent radiation propagation use coordinates appropriate for (approximate) rectilinear propagation. However, partially coherent radiation propagates throughout an angular spectrum.⁹ Therefore, polar coordinates are more appropriate than Cartesian coordinates to study partially coherent radiation propagation. Importantly, the derived results relax to the Huygens-Fresnel result for the special case of a coherent source, demonstrating equivalence with the previous coherent source analyses.¹⁰ Significantly, they also relax to the far-field coherence-angular distribution relations^{9,11} characterizing a partially coherent source for the special case of vacuum propagation. A simple physical picture of the atmospheric effects in terms of scattering functions is an additional benefit provided by this approach.

To illustrate the effects of range, propagation angle, source size and coherence, and strength of turbulence on the spatial coherence (second moment) predicted by this analysis, simplifying approximations are made which facilitate closed-form solutions. The phase of the predicted mutual coherence function (MCF) changes with field-point separation at off-normal propagation angles. This effect has not been previously predicted because of assumed axial propagation (including the speckle analysis of Lee *et al.*⁷). Numerical results for the MCF amplitude and phase coherence lengths are calculated and depicted.

THEORETICAL FOUNDATION

A monochromatic (spatially) partially coherent source is assumed that occupies a portion of the x - y plane (Fig 1). Physical embodiments of such a source are laser-illuminated diffusers or rough surfaces. Restricting the analysis to the scalar problem¹² for simplicity and ease of comparison with previous work and denoting the vectors $\mathbf{r} = (x, y, 0)$ and $\mathbf{P} = (x, y, z)$, and the wave number k , the scalar field at \mathbf{P} (resulting from the source propagating through a turbulent medium) is given by

$$U^{\text{turb}}(\mathbf{P}) = \frac{-z}{2\pi} \int \int_{-\infty}^{\infty} d^2\mathbf{r} U(\mathbf{r}) \left(\frac{ik}{|\mathbf{r} - \mathbf{P}|^2} - \frac{1}{|\mathbf{r} - \mathbf{P}|^3} \right) \times \exp[ik|\mathbf{r} - \mathbf{P}| + \psi(\mathbf{P}, \mathbf{r})], \quad (1)$$

where $\psi(\mathbf{P}, \mathbf{r})$ represents the phase and log-amplitude variation from the vacuum solution for a spherical wave propagating from \mathbf{r} to \mathbf{P} . Equation (1) follows from an extension of the "self-consistent" Rayleigh-Sommerfeld solution^{13,14}

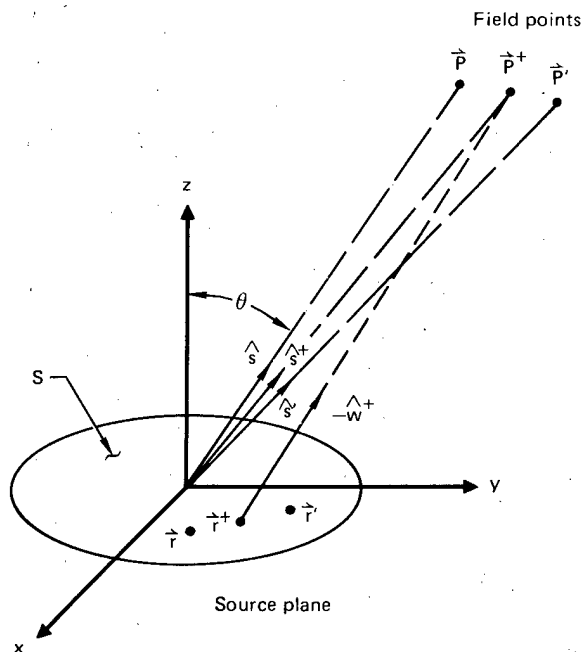


FIG. 1. Geometry relating the source S the source-points \mathbf{r} , \mathbf{r}' , \mathbf{r}^+ , the field points \mathbf{P} , \mathbf{P}' , \mathbf{P}^+ , the unit field point direction vectors $\hat{\mathbf{s}}$, $\hat{\mathbf{s}}'$, $\hat{\mathbf{s}}^+$, and the unit vector $\hat{\mathbf{w}} = (\mathbf{r}^+ - \mathbf{P}^+)/|\mathbf{r}^+ - \mathbf{P}^+|$.

for the scalar field at \mathbf{P} resulting from the aperture field $U(\mathbf{r})$. The extension of this solution to turbulent medium propagation consists essentially of the additional complex phase term $\psi(\mathbf{P}, \mathbf{r})$ following identical arguments presented in Refs. 8 and 15. Assuming that the source-field distribution is relatively large with respect to a wavelength and restricting the analysis to propagation distances, $R = (x^2 + y^2 + z^2)^{1/2}$, that are much greater than a typical source dimension, Eq. (1) can be written

$$U^{\text{turb}}(\mathbf{P}) \cong -\frac{\cos\theta ik}{2\pi R} \int \int_{-\infty}^{\infty} d^2\mathbf{r} U(\mathbf{r}) e^{ik|\mathbf{r} - \mathbf{P}| + \psi(\mathbf{r}, \mathbf{P})} \quad (2)$$

to an excellent approximation, where θ is the angle subtended between \mathbf{P} and the z axis. Denoting the average over the ensemble of all source and turbulent medium configurations by angle brackets $\langle \rangle$, the field-point MCF can be written

$$\Gamma^{\text{turb}}(\mathbf{P}, \mathbf{P}') = \langle U^{\text{turb}}(\mathbf{P}) U^{*\text{turb}}(\mathbf{P}') \rangle = \frac{\cos\theta \cos\theta' k^2}{(2\pi)^2 RR'} \int \int_{-\infty}^{\infty} \int \int_{-\infty}^{\infty} d^2\mathbf{r} d^2\mathbf{r}' \Gamma_s(\mathbf{r}, \mathbf{r}') \times F(\mathbf{r}, \mathbf{r}', \mathbf{P}, \mathbf{P}') \exp[ikL(\mathbf{r}, \mathbf{r}', \mathbf{P}, \mathbf{P}')], \quad (3)$$

where

$$\Gamma_s(\mathbf{r}, \mathbf{r}') = \langle U(\mathbf{r}) U^*(\mathbf{r}') \rangle, \quad (4)$$

$$F(\mathbf{r}, \mathbf{r}', \mathbf{P}, \mathbf{P}') = \langle \exp[\psi(\mathbf{r}, \mathbf{P}) + \psi^*(\mathbf{r}', \mathbf{P}')] \rangle, \quad (5)$$

$$L(\mathbf{r}, \mathbf{r}', \mathbf{P}, \mathbf{P}') = |\mathbf{r} - \mathbf{P}| - |\mathbf{r}' - \mathbf{P}'|, \quad (6)$$

and the order of integration and ensemble averaging has been interchanged. Note that the averages of the source-field and medium propagation variables are separable because these are presumably independent random processes. Denoting unit vectors $\hat{\mathbf{s}}$ and $\hat{\mathbf{s}}'$ in the respective directions \mathbf{P} and \mathbf{P}' , the following sum and difference coordinates are defined:

$$\mathbf{r}^+ = (\mathbf{r} + \mathbf{r}')/2 \quad \text{and} \quad \mathbf{r}^- = \mathbf{r} - \mathbf{r}', \quad (7)$$

$$\mathbf{P}^+ = (\mathbf{P} + \mathbf{P}')/2 \quad \text{and} \quad \mathbf{P}^- = \mathbf{P} - \mathbf{P}', \quad (8)$$

$$\hat{s}^+ = (\hat{s} + \hat{s}')/2 \quad \text{and} \quad \hat{s}^- = \hat{s} - \hat{s}', \quad (9)$$

$$R^+ = (R + R')/2 \quad \text{and} \quad R^- = R - R', \quad (10)$$

$$\theta^+ = (\theta + \theta')/2 \quad \text{and} \quad \delta = \theta - \theta'. \quad (11)$$

Appendix A demonstrates that the phase factor $L(\mathbf{r}, \mathbf{r}', \mathbf{P}, \mathbf{P}')$ is approximately given by

$$L(\mathbf{r}, \mathbf{r}', \mathbf{P}, \mathbf{P}') \cong (\mathbf{r} \cdot \mathbf{r}^+/R^+ - \mathbf{r}^- \cdot \hat{s}^+ - \mathbf{r}^+ \cdot \hat{s}^- + R^-). \quad (12)$$

The ensemble-averaged medium propagation factor $F(\mathbf{r}, \mathbf{r}', \mathbf{P}, \mathbf{P}')$ is recognized as the two(point)-source spherical-wave mutual coherence function. Assuming isoplanicity, the variable dependence of the two-source, spherical wave MCF is

$$F(\mathbf{r}, \mathbf{r}', \mathbf{P}, \mathbf{P}') = F(\mathbf{r}^-, \mathbf{P}^-; R^+). \quad (13)$$

The field point MCF therefore can be written

$$\begin{aligned} \Gamma^{\text{turb}}(\mathbf{P}^+, \mathbf{P}^-) &\cong \frac{k^2 \cos^2 \theta^+}{(2\pi R^+)^2} \frac{e^{ikR^-}}{[1 - (R^-/2R^+)^2]} \\ &\times \int \int_{-\infty}^{\infty} \int \int_{-\infty}^{\infty} d^2\mathbf{r}^+ d^2\mathbf{r}^- \Gamma_s(\mathbf{r}^+, \mathbf{r}^-) F(\mathbf{r}^-, \mathbf{P}^-; R^+) \\ &\times \exp[ik(\mathbf{r}^- \cdot \mathbf{r}^+/R^+ - \mathbf{r}^- \cdot \hat{s}^+ - \mathbf{r}^+ \cdot \hat{s}^-)], \quad (14) \end{aligned}$$

assuming small field-point-difference angles δ . Defining the function

$$\begin{aligned} G(\mathbf{r}^-, \mathbf{P}^-) \\ \cong 1/A \int \int_{-\infty}^{\infty} d^2\mathbf{r}^+ \Gamma_s(\mathbf{r}^+, \mathbf{r}^-) e^{i(k\mathbf{r}^+ \cdot (\mathbf{r}^-/R^- - \hat{s}^-))} \quad (15) \end{aligned}$$

as the generalized, two-field-point, source coherence (the rationale for this appellation is provided below), where

$$A = \int_S d^2\mathbf{r}^+ \quad (16)$$

is the source area; the field-point MCF is

$$\begin{aligned} \Gamma^{\text{turb}}(\mathbf{P}^+, \mathbf{P}^-) &= \frac{\Omega_s}{(2\pi)^2} \frac{e^{ikR^-} \cos^2 \theta^+}{[1 - (R^-/2R^+)^2]} \\ &\times \int \int_{-\infty}^{\infty} d^2(k\mathbf{r}^-) e^{-i(k\mathbf{r}^-) \cdot \hat{s}^+} G(\mathbf{r}^-, \mathbf{P}^-) F(\mathbf{r}^-, \mathbf{P}^-), \quad (17) \end{aligned}$$

where

$$\Omega_s = A(R^+)^{-2} \quad (18)$$

is the solid angle subtended by the source at range R^+ . It is noted that for vacuum propagation

$$F(\mathbf{r}^-, \mathbf{P}^-)|_{\text{vacuum}} = 1 \quad (19)$$

so that the field-point MCF reduces to

$$\begin{aligned} \Gamma^{\text{vac}}(\mathbf{P}^+, \mathbf{P}^-) &= \frac{\Omega_s}{(2\pi)^2} \frac{e^{ikR^-} \cos^2 \theta^+}{[1 - (R^-/2R^+)^2]} \\ &\times \int \int_{-\infty}^{\infty} d^2(k\mathbf{r}^-) e^{-i(k\mathbf{r}^-) \cdot \hat{s}^+} G(\mathbf{r}^-, \mathbf{P}^-) \quad (20) \end{aligned}$$

for vacuum propagation. Spatial source-plane Fourier transforms of the generalized two-field-point source coherence and the two-source spherical-wave MCF are now defined,

$$\hat{G}(\hat{\xi}, \mathbf{P}^-) \equiv \int \int_{-\infty}^{\infty} d^2(k\mathbf{r}^-) e^{-i(k\mathbf{r}^-) \cdot \hat{\xi}} G(\mathbf{r}^-, \mathbf{P}^-), \quad (21)$$

and

$$\hat{F}(\hat{\xi}, \mathbf{P}^-) \equiv \int \int_{-\infty}^{\infty} d^2(k\mathbf{r}^-) e^{-i(k\mathbf{r}^-) \cdot \hat{\xi}} F(\mathbf{r}^-, \mathbf{P}^-). \quad (22)$$

Because the vector $\hat{\xi}$ corresponds to a unit vector direction, the Fourier-transformed generalized two-field-point source coherence can be expressed

$$\begin{aligned} \hat{G}(\hat{\xi}, \mathbf{P}^-) &= \frac{(2\pi)^2 [1 - (R^-/2R^+)^2]}{\Omega_s (1 - \xi_x^2 - \xi_y^2)} \\ &\times e^{-ikR^-} \Gamma^{\text{vac}}(R^+, \hat{\xi}, \mathbf{P}^-) \quad (23) \end{aligned}$$

using Eq. (20) for the vacuum MCF. Thus the turbulent medium MCF can be expressed in terms of the vacuum MCF as

$$\begin{aligned} \Gamma^{\text{turb}}(\mathbf{P}^+, \mathbf{P}^-) &= \frac{\cos^2 \theta^+}{(2\pi)^2} \\ &\times \int \int_{-\infty}^{\infty} d^2\hat{\xi} \frac{\Gamma^{\text{vac}}(R^+, \hat{\xi}, \mathbf{P}^-)}{(1 - \xi_x^2 - \xi_y^2)} \hat{F}(\hat{s}^+ - \hat{\xi}, \mathbf{P}^-) \quad (24) \end{aligned}$$

using Eqs. (17), (22), (23) and the convolution theorem of Fourier transformation. Note that for vacuum propagation

$$\hat{F}(\hat{\xi}, \mathbf{P}^-)|_{\text{vacuum}} = (2\pi)^2 \delta(\hat{\xi}), \quad (25)$$

using Eq. (19), so that

$$\begin{aligned} \Gamma^{\text{turb}}(\mathbf{P}^+, \mathbf{P}^-)|_{\text{vacuum}} &= \cos^2 \theta^+ \\ &\times \int \int_{-\infty}^{\infty} d^2\hat{\xi} \frac{\Gamma^{\text{vac}}(R^+, \hat{\xi}, \mathbf{P}^-)}{(1 - \xi_x^2 - \xi_y^2)} \delta(\hat{s}^+ - \hat{\xi}) = \Gamma^{\text{vac}}(\mathbf{P}^+, \mathbf{P}^-), \quad (26) \end{aligned}$$

providing a check on the self-consistency of Eq. (24).

Partial validation of the above equations is obtained by examining relevant limiting cases. Clearly, as the source becomes perfectly coherent, the radiation propagates primarily along the z axis.⁹ Thus, field-point vectors (\mathbf{p} and \mathbf{p}') that are transverse to the z axis can be defined to parameterize the field point separations. The unit direction vectors \hat{s} and \hat{s}' are then given by

$$\hat{s} \cong \mathbf{p}/z + \hat{k}$$

and

$$\hat{s}' \cong \mathbf{p}'/z' + \hat{k}, \quad (27)$$

where \hat{k} is a unit vector along the z axis. Substitution of Eq. (27) in Eq. (14) then yields¹⁶

$$\begin{aligned} \Gamma^{\text{turb}}(\mathbf{p}, \mathbf{p}') &\cong k^2/(2\pi z)^2 \\ &\times \int \int_{-\infty}^{\infty} \int \int_{-\infty}^{\infty} d^2\mathbf{r}^+ d^2\mathbf{r}^- U(\mathbf{r}^+ + \mathbf{r}^-/2) \\ &\times U^*(\mathbf{r}^+ - \mathbf{r}^-/2) F(\mathbf{r}^-, \mathbf{p}^-) \\ &\times \exp[ik(\mathbf{r}^+ - \mathbf{p}^+) \cdot (\mathbf{r}^- - \mathbf{p}^-)], \quad (28) \end{aligned}$$

where

$$\mathbf{p}^+ = (\mathbf{p} + \mathbf{p}')/2, \quad \mathbf{p}^- = \mathbf{p} - \mathbf{p}',$$

and the coherent form for the source MCF¹⁷ has been used together with the fact that $\cos^2 \theta^+ \cong 1$ and the assumption that

$z = z'$. Equation (28) is recognized as the turbulent medium MCF predicted by the extended Huygens-Fresnel principle for a coherent source.⁵

Examining the far-field propagation of the radiation intensity *in vacuo*, Eq. (14) reduces to

$$J^{\text{vac}}(\mathbf{P}^+) |_{\text{far-field}} = \Gamma^{\text{turb}}(\mathbf{P}^+, 0) |_{\text{vacuum, far-field}} = \frac{k^2 \cos^2 \theta^+}{(2\pi R^+)^2} \times \int \int_{-\infty}^{\infty} \int \int_{-\infty}^{\infty} d^2 \mathbf{r}^+ d^2 \mathbf{r}^- \Gamma_s(\mathbf{r}^+, \mathbf{r}^-) e^{-ik\mathbf{r}^- \cdot \hat{s}^+}. \quad (29)$$

Assuming that the source is statistically homogeneous (in the same sense described in Ref. 9), Eq. (29) reduces to

$$J^{\text{vac}}(\mathbf{P}^+) |_{\text{far-field}} = \frac{k^2 \cos^2 \theta^+}{(2\pi R^+)^2} A \hat{\Gamma}_s(k\hat{s}_\perp^+), \quad (30)$$

where

$$\hat{\Gamma}_s(k\hat{s}_\perp^+) = \int \int_{-\infty}^{\infty} d^2 \mathbf{r}^- e^{-ik\mathbf{r}^- \cdot \hat{s}^+} \Gamma_s(\mathbf{r}^-), \quad (31)$$

the Fourier transform of the source mutual coherence, where \hat{s}_\perp is the projection of \hat{s} on the x - y plane. Equation (30) is equivalent to the relationship derived by Wolf and Carter⁹ relating the far-field intensity angular distribution and the source coherence. Furthermore, an equivalent statement of the far-field van-Cittert-Zernike theorem can be derived using Eqs. (14) and (30), employing the same procedures described in the reference cited in Ref. 12.

Returning to the problem of turbulent medium propagation, it is noted that the radiation intensity in the turbulent medium is given by [Eq. (24)],

$$J^{\text{turb}}(\mathbf{P}^+) = \Gamma^{\text{turb}}(\mathbf{P}^+, 0) = \frac{\cos^2 \theta^+}{(2\pi)^2} \times \int \int_{-\infty}^{\infty} d^2 \xi \frac{J^{\text{vac}}(R^+ \xi)}{(1 - \xi_x^2 - \xi_y^2)} \tilde{M}(\hat{s}^+ - \xi), \quad (32)$$

where

$$\tilde{M}(\xi) = \int \int_{-\infty}^{\infty} d^2(k\mathbf{r}^-) e^{-i(k\mathbf{r}^-) \cdot \xi} F(\mathbf{r}^-, 0) \quad (33)$$

is the Fourier-transformed mutual coherence function for a spherical wave propagating in the turbulent medium. Equation (32) lends itself to a simple physical interpretation since it is exactly the same form that results from postulating a scattering function that describes the angular deviation of the vacuum radiant intensity resulting from propagation in the turbulent medium. The total intensity in any given direction is then the convolution of the vacuum intensity distribution with the postulated scattering function. Clearly, in this case, the scattering function is given by the Fourier-transformed, spherical-wave MCF divided by the factor $(1 - \xi_x^2 - \xi_y^2)$. Analogously, Eq. (24) expresses the turbulent medium MCF in terms of the vacuum MCF angular distribution (for a fixed field-point separation vector \mathbf{P}^-) convolved with a pseudo-scattering function that describes the average vector angular deviation of the vacuum MCF (again with a fixed field-point separation vector \mathbf{P}^-) resulting from propagation in the turbulent medium. In this case the pseudo-scattering function is given by the Fourier-transformed, two-source, spherical wave MCF divided by the factor $(1 - \xi_x^2 - \xi_y^2)$. To complete the physical interpretation of the above equations,

it is noted that the far-field expression for $G(\mathbf{r}^-, \mathbf{P}^-)$ [Eq. (15)] with zero field-point separation is

$$G(\mathbf{r}^-, 0) |_{\text{far-field}} = \frac{1}{A} \int \int_{-\infty}^{\infty} d^2 \mathbf{r}^+ \Gamma_s(\mathbf{r}^+, \mathbf{r}^-), \quad (34)$$

which is the spatial average of the source mutual coherence function. Thus, the general function $G(\mathbf{r}^-, \mathbf{P}^-)$ is the generalization of the average source mutual coherence that results from considering separate field points and near-field ranges. Hence the appellation of the generalized, two-field-point source coherence for the function $G(\mathbf{r}^-, \mathbf{P}^-)$ results. Equation (17) provides a mathematical statement of the propagation of the (generalized) source coherence in a turbulent medium. The Fourier-transform relations that have been noted permit an interpretation of this expression in terms of scattering functions.

CALCULATIONS

To perform specific calculations of the MCF obtained from a partially coherent source propagating through the turbulent atmosphere, it is necessary to specify the generalized, two-source spherical-wave MCF, $F(\mathbf{r}^-, \mathbf{P}^-)$, or equivalently, the pseudo-scattering function $\hat{F}(\xi, \mathbf{P}^-)$. If the statistics of the complex phase ψ are Gaussian, then the two-source spherical-wave MCF is given by¹⁸

$$F(\mathbf{r}^-, \mathbf{P}^-) = \exp \left[-\frac{1}{2} D_\psi(\mathbf{r}^-, \mathbf{P}^-) \right], \quad (35)$$

where

$$D_\psi(\mathbf{r}^-, \mathbf{P}^-) = D_\chi(\mathbf{r}^-, \mathbf{P}^-) + D_S(\mathbf{r}^-, \mathbf{P}^-), \quad (36)$$

the sum of the log-amplitude (D_χ) and phase (D_S), two-source spherical-wave structure functions. Assuming a Kolmogorov turbulence spectrum and weak turbulence the complex phase, two-source, spherical-wave structure function is given by^{19,20}

$$D_\psi(\mathbf{r}^-, \mathbf{P}^-) = 2.91k^2 R^+ \int_0^1 dt C_n^2(R^+ t) |t\mathcal{P}(\mathbf{P}^-) + (1-t)\mathcal{P}(\mathbf{r}^-)|^{5/3}, \quad (37)$$

where $C_n^2(R)$ is the refractive index structure constant, radial changes in the complex phase ψ are ignored (these are small for small R^-), and the operator $\mathcal{P}(\mathbf{x})$ projects the vector \mathbf{x} onto a plane that is transverse to the \mathbf{P}^+ direction. Equation (37) assumes that the absolute values of the projected vector differences $|\mathcal{P}(\mathbf{r}^-)|$ and $|\mathcal{P}(\mathbf{P}^-)|$ are much less than a Fresnel zone length, $(2\pi R^+/k)^{1/2}$. Although the integral of Eq. (37) cannot be integrated exactly, approximate expansions can be obtained and used with Eq. (35) and the preceding development to perform numerical calculations of the MCF of a partially coherent source. However, these procedures are complicated and permit little physical understanding of the propagation characteristics as a function of the variables of interest. Analytical calculations of the MCF are permitted by approximating the five-thirds power of the projected vector sum in Eq. (37) by the square. Normalizing the resultant two-source spherical-wave MCF to the correct five-thirds law spherical-wave coherence length at the e^{-1} point yields

$$F(\mathbf{r}^-, \mathbf{P}^-) \cong \exp \left[-3\rho_0^{-2} \int_0^1 dt |t\mathcal{P}(\mathbf{P}^-) + (1-t)\mathcal{P}(\mathbf{r}^-)|^2 \right], \quad (38)$$

so that

$$M(\rho) = F[0, \rho = |\mathcal{P}(\mathbf{P}^-)|] \cong e^{-(\rho/\rho_0)^2}, \quad (39)$$

where

$$\rho_0 = [3/8 \times 1.455k^2R + C_n^2]^{-3/5}, \quad (40)$$

assuming homogeneous turbulence. Appendix B provides a calculation of the MCF of a uniform coherent source using the approximations of Eqs. (38)–(40) and the preceding development. It is noteworthy that the plane-wave coherence length predicted by this approximation ($0.58\rho_0$) is in reasonable agreement with the five-thirds law prediction ($0.56\rho_0$). Calculations are also provided in Appendix B for the Fourier transform of the uniform source mutual coherence in terms of a dimensionless spatial frequency spectrum V and a dimensionless spatial frequency $\tilde{\chi}$. The predicted spectrum of the mutual coherence, resulting from the quadratic approximation, Eqs. (38)–(40), is plotted in Fig. 2 along with experimental data of Artem'ev and Gurvich²¹ and three different calculations of a modified Kolmogorov spectrum²¹ corresponding to three different values of the inner scale of turbulence. Significantly, the approximate quadratic spectrum is within 1 dB of the experimental data over the range of frequencies plotted and is closer to the measured data than two of the modified Kolmogorov spectra for the highest measured spatial frequencies. Because the quadratic approximation is in reasonable agreement with available MCF spectral data, it is employed for subsequent calculations to obtain closed-form analytical expressions for the MCF of radiation propagating from partially coherent sources. It is expected that although detailed predicted behavior may deviate somewhat from that obtained from the five-thirds law MCF, the predicted trends with respect to the various variables of interest should be the same as those obtained from

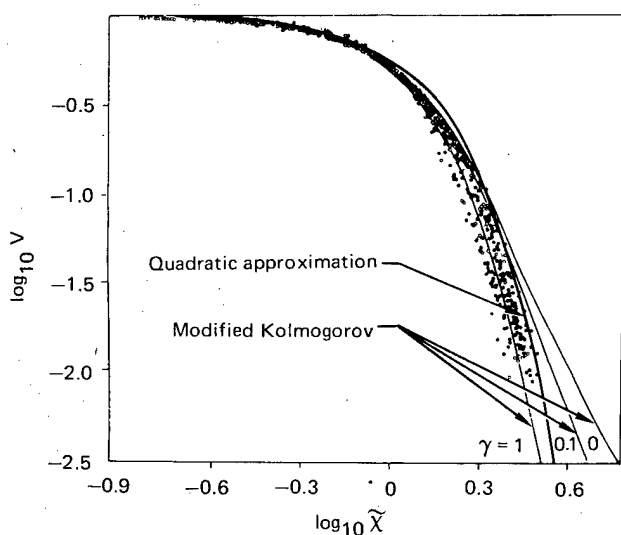


FIG. 2. Experimental spatial spectra of the coherence function obtained by Artem'ev and Gurvich²¹ (open circles) compared with predictions derived from a modified Kolmogorov turbulence spectrum (solid lines) and the quadratic approximation (heavy solid line) discussed in Appendix B.

the more accurate description of the atmospheric, spherical-wave structure function.

The form of the source mutual coherence function that will be used for the subsequent investigation is

$$\Gamma_s(\mathbf{r}^+, \mathbf{r}^-) = I_s \pi \exp[-(|\mathbf{r}^-|^2/\rho_e^2 + |\mathbf{r}^+|^2/L^2)]. \quad (41)$$

Equation (41) is particularly suitable for this investigation because when

$$\rho_e = 2L,$$

$$\Gamma_s(\mathbf{r}, \mathbf{r}') = I_s \pi \exp[-(2L)^{-2}(|\mathbf{r}|^2 + |\mathbf{r}'|^2)], \quad (42)$$

which is the form of the source coherence for a coherent Gaussian beam. However, when $\rho_e < 2L$, the source coherence is similar to that obtained from specular glints from a laser-illuminated rough surface with an equivalent rms surface slope given by

$$s_{\text{eff}} = \lambda/\pi\rho_e. \quad (43)$$

Thus variation of the parameter ρ_e simulates laser reflectance (TEM₀₀) from a surface with a variable surface roughness. The similarity of the source MCF with that of the rough surface is demonstrated by noting that the far-field vacuum intensity distribution associated with the assumed source coherence is [Eq. (29)]

$$J^{\text{vac}}(\theta)|_{\text{far-field}} = (I_s \Omega_s/4) \cos^2\theta^+ (k\rho_e)^2 \times \exp[-(k\rho_e/2)^2 \sin^2\theta] \quad (44)$$

using

$$A = \int \int_{-\infty}^{\infty} d^2\mathbf{r}^+ e^{-|\mathbf{r}^+|^2/L} = \pi L^2. \quad (45)$$

Recalling the Fourier-transform relationship between the far-field intensity angular distribution and the source coherence [Eq. (30) and Refs. 9 and 11] and noting that the angular distribution of the radiation intensity scattered by specular glints of a rough surface is²²

$$J(P^+)|_{\text{specular glints}} \sim (\sec^4\theta/s^2) \exp(-\tan^2\theta/s^2), \quad (46)$$

where s is the rms surface slope, the stated equivalence [Eq. (43)] is established in the small-angle approximation.

Before proceeding with calculations of the turbulent medium propagation of radiation derived from the assumed partially coherent source [Eq. (41)], it is instructive to examine vacuum propagation of the mutual coherence. The vacuum MCF predicted by Eq. (20) for the source MCF of Eq. (41) is

$$\begin{aligned} \Gamma^{\text{vac}}(\mathbf{P}^+, \mathbf{P}^-) &= \frac{J^{\text{vac}}(\theta^+)|_{\text{far-field}}}{[1 - (R^-/2R^+)^2]} e^{ikR^- \mathcal{R}} \left(\frac{R_{\text{ff}}}{R^+} \right) \\ &\times \exp \left[- \left(\frac{R_{\text{ff}}}{\rho_e} \right)^2 \mathcal{R} \left(\frac{R_{\text{ff}}}{R^+} \right) (\beta^2 + \cos^2\theta^+ \delta^2) \right] \\ &\times \exp \left\{ \left(\frac{R_{\text{ff}}}{L} \right)^2 \sin^2\theta^+ \left[1 - \mathcal{R} \left(\frac{R_{\text{ff}}}{R^+} \right) \right] \right\} \\ &\times \exp \left[ikR_{\text{ff}}^2 \mathcal{R} \left(\frac{R_{\text{ff}}}{R^+} \right) (R^+)^{-1} (\beta s_x^+ - \delta s_y^+ \cos\theta^+) \right], \quad (47) \end{aligned}$$

where

$$\beta \equiv \omega \sin\theta^+, \quad (48)$$

$$s_x^+ = \sin\theta^+ \sin\phi, \quad (49a)$$

$$s_y^+ = \sin\theta^+ \cos\phi, \quad (49b)$$

$$\mathcal{R}(R_{\text{ff}}/R^+) = [1 + (R_{\text{ff}}/R^+)^2]^{-1}, \quad (50)$$

$$R_{\text{ff}} = kL\rho_e/2, \quad (51)$$

ω is the azimuthal difference angle between the two field-point coordinates, and ϕ is the azimuthal angle subtended between the y axis and the projection of the \hat{s}^+ vector on the x - y plane. Note that the radiance intensity predicted by Eq. (47) (i.e., $\delta = \beta = R^- = 0$) approaches the predicted far-field intensity when $R^+ \gg R_{\text{ff}}$. Therefore R_{ff} is interpreted as the equivalent far-field range for a partially coherent source with a Gaussian coherence function. This interpretation is supported by the following observations. When the source coherence length is equal to the source dimension ($2L$), the equivalent far-field range is ($R_{\text{ff}} = 2\pi L^2/\lambda$), within a factor of 1.27 of the far-field range customarily predicted for a uniformly illuminated aperture [$2(2L)^2/\lambda$]. However, when the coherence length of the source is on the order of the wavelength, the equivalent far-field range decreases to the order of the source dimension (πL). It is well known that valid measurements of the far-field angular distributions of incoherent sources can be performed at close range. The equivalent far-field range parameter R_{ff} critically affects the range dependence of the vacuum MCF and the turbulent medium MCF calculated below. As the far-field range is exceeded, the MCF predicted by Eq. (47) approaches the prediction of the far-field van-Cittert-Zernike theorem for the assumed source irradiance

$$\begin{aligned} \Gamma^{\text{turb}}(\mathbf{P}^+, \mathbf{P}^-) &= \frac{J^{\text{vac}}(\theta^+) |_{\text{far-field}}}{[1 - (R^-/2R^+)^2]} \frac{e^{ikR^-}}{(QQ')^{1/2}} \exp\left(-\beta^2 \left\{ \left(\frac{R^+}{\rho_0}\right)^2 \left[1 - \frac{1}{4} \left(\frac{\rho_e}{\rho_0}\right)^2 Q^{-1}\right] + \left(\frac{R_{\text{ff}}}{\rho_e}\right)^2 Q^{-1}\right\}\right) \\ &\times \exp\left(-\delta^2 \left\{ \left(\frac{R^+}{\rho_0}\right)^2 \left[1 - \frac{1}{4} \left(\frac{\rho_e}{\rho_0}\right)^2 \cos^2\theta + Q^{-1}\right] + \left(\frac{R_{\text{ff}}}{\rho_e}\right)^2 \cos^2\theta + [1 - (Q-1)Q^{-1}]\right\}\right) \\ &\times \exp\left\{ \left(\frac{R_{\text{ff}}}{L}\right)^2 [\sin^2\theta + (s_x^+)^2 Q^{-1} - (s_y^+)^2 Q^{-1}] \right\} \\ &\times \exp ikR^+ \left\{ \beta s_x^+ \left[\left(\frac{R_{\text{ff}}}{R^+}\right)^2 + \frac{1}{2} \left(\frac{\rho_e}{\rho_0}\right)^2 \right] Q^{-1} - \delta s_y^+ \left[\left(\frac{R_{\text{ff}}}{R^+}\right)^2 + \frac{1}{2} \left(\frac{\rho_e}{\rho_0}\right)^2 \right] \cos\theta + Q^{-1} \right\}, \quad (55) \end{aligned}$$

where

$$Q = [1 + (R_{\text{ff}}/R^+)^2 + (\rho_e/\rho_0)^2] \quad (56a)$$

and

$$Q' = [1 + (R_{\text{ff}}/R^+)^2 + (\rho_e/\rho_0)^2 \cos^2\theta]. \quad (56b)$$

It can be verified by inspection that Eq. (55) reduces to the vacuum result as the atmospheric turbulence goes to zero (i.e., $\rho_0 \rightarrow \infty$). It is noteworthy that the ratio of the source coherence length to the atmospheric coherence length (ρ_c/ρ_0) is a

$$\begin{aligned} \gamma^{\text{turb}}(P^+, P^-) &= \frac{\Gamma^{\text{turb}}(\mathbf{P}, \mathbf{P}')}{[\Gamma^{\text{turb}}(\mathbf{P}, \mathbf{P})\Gamma^{\text{turb}}(\mathbf{P}', \mathbf{P}')]^{1/2}} \cong \frac{\Gamma^{\text{turb}}(\mathbf{P}^+, \mathbf{P}^-)}{\Gamma^{\text{turb}}(\mathbf{P}^+, 0)} \\ &= \frac{e^{ikR^-}}{[1 - (R^-/2R^+)^2]} \exp\left(-\delta^2 \left\{ \left(\frac{R^+}{\rho_0}\right)^2 \left[1 - \frac{1}{4} \left(\frac{\rho_e}{\rho_0}\right)^2 \cos^2\theta + Q^{-1}\right] \right. \right. \\ &\left. \left. + \left(\frac{R_{\text{ff}}}{\rho_e}\right)^2 \cos^2\theta + [1 - (Q-1)Q^{-1}]\right\}\right) \exp\left\{-i(kR^+)\delta \sin\theta \cos\theta \left[\left(\frac{R_{\text{ff}}}{R^+}\right)^2 + \frac{1}{2} \left(\frac{\rho_e}{\rho_0}\right)^2 \right] Q^{-1}\right\} \quad (57) \end{aligned}$$

for small field-point separation angles δ .

A further simplification results from defining the degree of coherence as

$$\begin{aligned} \gamma(\theta^+, R^+, \delta, R^-) &= T(\theta^+, R^+, \delta) e^{i\alpha(\theta^+, R^+)\delta} \\ &\times e^{ikR^-} [1 - (R^-/2R^+)^2]^{-1}, \quad (58) \end{aligned}$$

distribution. Because the phase difference of the field points [predicted by Eq. (47)] increases with increasing source coherence length, the phase portion of the predicted MCF results from deterministic beam-spreading effects.

Appendix C provides a derivation of the generalized two-source spherical-wave mutual coherence function $F(\mathbf{r}^-, \mathbf{P}^-, R^+)$ [using the approximations of Eqs. (38)–(40)] and the pseudo-scattering function $\hat{F}(\xi, \mathbf{P}^-; \mathbf{R}^+)$. The derived results are

$$F(\mathbf{r}^-, \mathbf{P}^-) = \exp\{- (R^+/\rho_0)^2 [(b + \beta)^2 + (c - \delta)^2 + c\delta - b\beta]\}, \quad (52)$$

where

$$b = x^-/R^+, \quad c = y^- \cos\theta^+/R^+, \quad (53)$$

$$\begin{aligned} \hat{F}(\xi, \mathbf{P}^-, R^+) &= \pi(k\rho_0)^2 \sec\theta^+ \exp\{-\frac{3}{4}(R^+/\rho_0)^2(\beta^2 + \delta^2)\} \\ &\times \exp\{-\frac{1}{4}(k\rho_0)^2[\xi_x^2 + \xi_y^2 \sec^2\theta]\} \\ &\times \exp[i(kR^+/2)(\xi_x\beta - \xi_y\delta \sec\theta)]. \quad (54) \end{aligned}$$

Employing Eq. (52) with Eqs. (17) and (15) [or equivalently Eq. (54) with Eqs. (24) and (47)] yields the following MCF resulting from the assumed partially coherent source [Eq. (41)] propagating through a (homogeneous) turbulent atmosphere:

critical parameter in determining the atmospheric effects of partially coherent radiation propagation. This observation is consistent with the analysis of Dunphy and Kerr,²³ who noted the critical nature of the ratio (L/ρ_0) for the propagation of coherent radiation. To facilitate analyses of the effects of various parameters on the predicted spatial coherence, it is convenient to normalize Eq. (55) to the field-point intensities (i.e., construct the degree of coherence function), choose an azimuthal plane of scattering ($\phi = 0$), and ignore the relatively uninteresting azimuthal dependence (i.e., choose $\beta = 0$). The degree of coherence is then

where the well-known radial dependence of the degree of coherence has been separated from the more interesting amplitude and phase dependence. Further, defining a magnitude correlation angle δ_e via the equation

$$T(\theta^+, R^+, \delta_e) \equiv e^{-1} T(\theta^+, R^+, 0) \equiv e^{-1} \quad (59)$$

and a $(\pi/4)$ phase correlation angle $\delta_{\pi/4}$ via a similar relation, i.e.,

$$\alpha(\theta^+, R^+) \delta_{\pi/4} \equiv \pi/4, \quad (60)$$

the respective magnitude and phase correlation angles follow from Eq. (57), i.e.,

$$\delta_e = \left\{ \left(\frac{R^+}{\rho_0} \right)^2 \left[1 - \frac{1}{4} \left(\frac{\rho_e}{\rho_0} \right)^2 \cos^2 \theta^+ Q'^{-1} \right] + \left(\frac{R_{ff}}{\rho_e} \right)^2 \cos^2 \theta^+ [1 - (Q-1)Q'^{-1}] \right\}^{-1/2} \quad (61)$$

and

$$\delta_{\pi/4} = \frac{\pi}{2} (kR^+)^{-1} \csc 2\theta^+ Q' \left[\left(\frac{R_{ff}}{R^+} \right)^2 + \frac{1}{2} \left(\frac{\rho_e}{\rho_0} \right)^2 \right]^{-1}. \quad (62)$$

Equations (61) and (62) define the e^{-1} and $\pi/4$ points, respectively, of the amplitude and phase angular field correlation. Corresponding coherence lengths are defined by the equations

$$\Delta_e = \delta_e R^+ \quad (63)$$

and

$$\Delta_{\pi/4} = \delta_{\pi/4} R^+. \quad (64)$$

Several observations can be made from inspection of the above equations. First, the phase coherence length becomes infinite for the axial and grazing propagation directions (i.e., the MCF phase remains constant regardless of the field-point separation). This behavior is consistent with all previous studies of coherent radiation propagation since phase effects have not been previously noted. In general, however, a finite-phase correlation length is predicted from this analysis because of beam spreading effects. Although the predicted phase coherence length (at nonaxial directions) increases as the range greatly exceeds the far-field range and the atmospheric coherence length greatly exceeds the source coherence length, these are generally incompatible simultaneous requirements for atmospheric incoherence unless the source is completely incoherent (i.e., δ correlated). Because perfectly incoherent sources are prohibited,²⁴ finite-phase coherence lengths are predicted at nonaxial directions in the atmosphere. The predicted angular dependence of the amplitude coherence length is also worthy of note. Clearly, as grazing angle propagation (90°) is approached, the effects on the source coherence length resulting from the finite coherence length are eliminated because of the $\cos^2 \theta^+$ factor multiplying these terms. The degree of coherence approaches that predicted for a spherical wave [Eq. (39)] in the polar plane, i.e., $\gamma \sim \exp[-(R^+ \delta)^2 / \rho_0^2]$, as the grazing geometry is approached. The physical reason for this phenomenon is that the projected source area approaches a line source as the grazing angle is approached and therefore becomes perfectly coherent in the transverse direction (i.e., the polar plane). Thus, a spherical wave MCF functional form is expected in the polar plane since the source is effectively a point source in this dimension.

To further explore the variable dependence of the MCF predicted by the above analysis, three-dimensional, computed, graphical results are employed. Calculated values of the amplitude and phase coherence lengths are plotted as the ordinate variation, while various combinations of the propa-

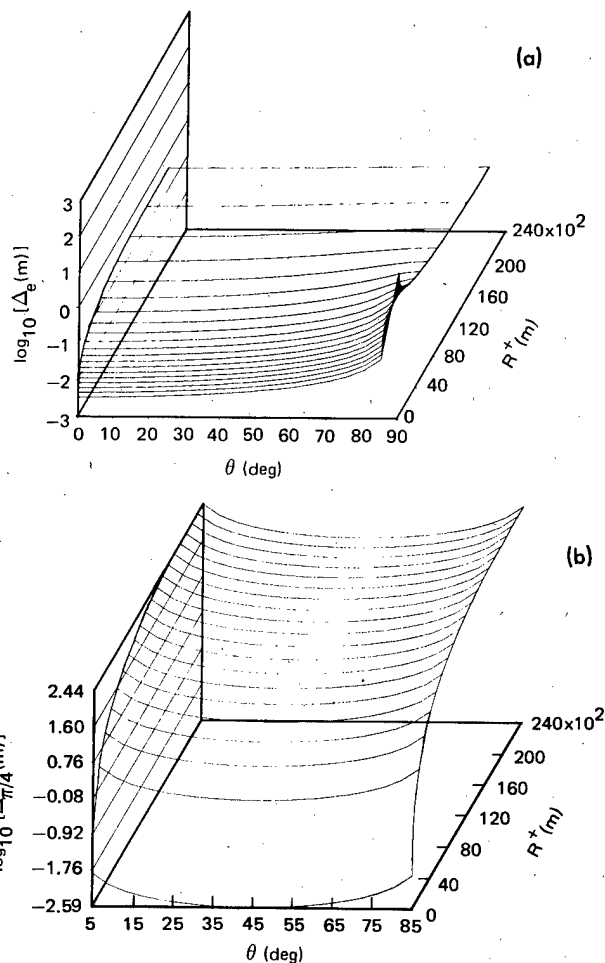


FIG. 3. Calculated values of the amplitude (a) and phase (b) coherence lengths as functions of the propagation angle (θ^+) and range (R^+). Fixed parameters are $\lambda = 10^{-5}$ m, $C_n^2 = 10^{-15}$ m^{-2/3}, $L = 10^{-1}$ m, and $\rho_e = 10^{-4}$ m.

gation parameters are used as independent variables along the x and y axes. Representative optical values of the fixed independent variables have been chosen for the subsequent illustrations.

Figure 3 illustrates the range and angle dependence of the amplitude and phase coherence lengths [Eqs. (63) and (64)] for a relatively incoherent source ($\rho_e = 10\lambda$) and moderate turbulence ($C_n^2 = 10^{-15}$ m^{-2/3}, $\lambda = 10^{-5}$ m). The aforementioned dependence of the apparent source coherence on the propagation direction is clearly illustrated by the amplitude coherence length dependence on the range and direction of propagation [Fig. 3(a)]. It is apparent that the amplitude coherence length is dominated by the finite source coherence (i.e., speckle dominated) for axial propagation [note that Δ_e is approximately proportional to $(R^+)^2$], whereas atmospheric effects begin to interact and dominate as the grazing propagation angle is approached [thus $\Delta_e \sim \rho_0 \sim (R^+)^{-3/5}$]. The phase coherence length is plotted only from 5° – 85° because it goes to infinity at the endpoints of the angular distribution (0° and 90°). The angular dependence of the phase coherence length is relatively unaffected by the range for the chosen fixed independent variables.

To illustrate the effects of the finite source coherence length

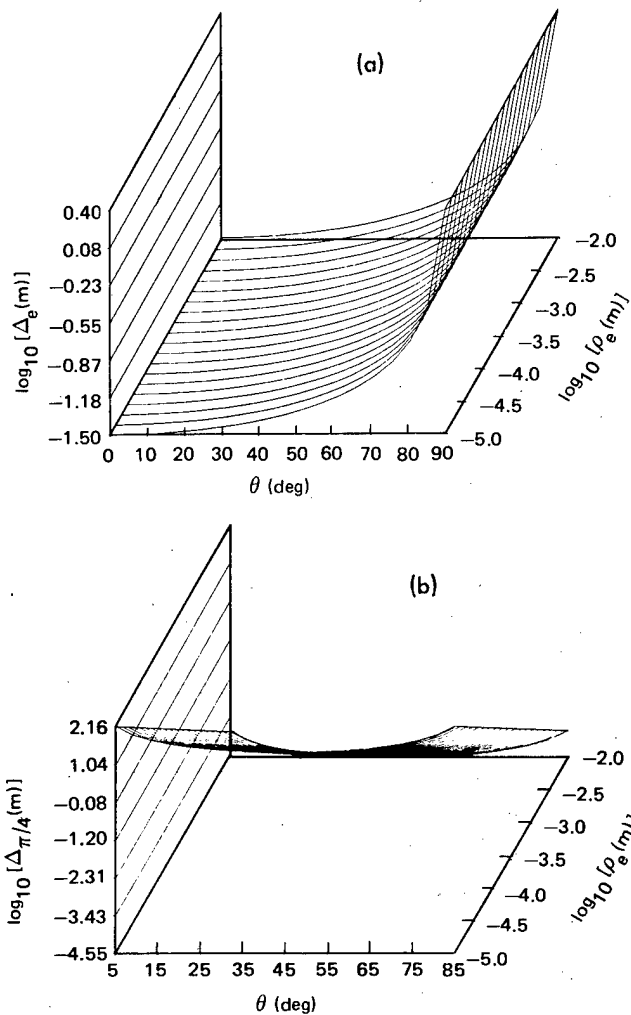


FIG. 4. Calculated values of the amplitude (a) and phase (b) coherence lengths as functions of the propagation angle (θ^+) and source coherence length (ρ_e). Fixed parameters are $\lambda = 10^{-5}$ m, $C_n^2 = 10^{-15}$ m $^{-2/3}$, $L = 10^{-1}$ m, and $R^+ = 10^3$ m.

on the predicted field coherence, Fig. 4 shows calculated values of the amplitude and phase coherence as functions of the propagation angle and source coherence (for relatively incoherent sources), while Fig. 5 depicts the same quantities as functions of the strength-of-turbulence (C_n^2) and source coherence for nearly coherent sources). Two different illustrations are employed because the vacuum intensity angular distribution [Eq. (44)] becomes strongly peaked in the axial direction for very coherent sources and hence angular plots of the predicted coherence lengths become meaningless for relatively coherent sources. It is evident from Fig. 4 that the angular distribution of the amplitude coherence length [Fig. 4(a)] is relatively unaffected by the source coherence length (for moderate turbulence and the range of coherence lengths plotted) although the phase coherence length decreases in proportion to the inverse square of the source coherence length. Because of the nearly rectilinear propagation characteristics of coherent sources Fig. 5 shows the phase and amplitude coherence lengths for nearly coherent sources at propagation angle of 10^{-3} rad and 0° , respectively, (recall that $\Delta_{\pi/4} \rightarrow \infty$ as $\theta^+ \rightarrow 0^\circ$) as a function of the refractive-index structure constant and the source coherence length. The

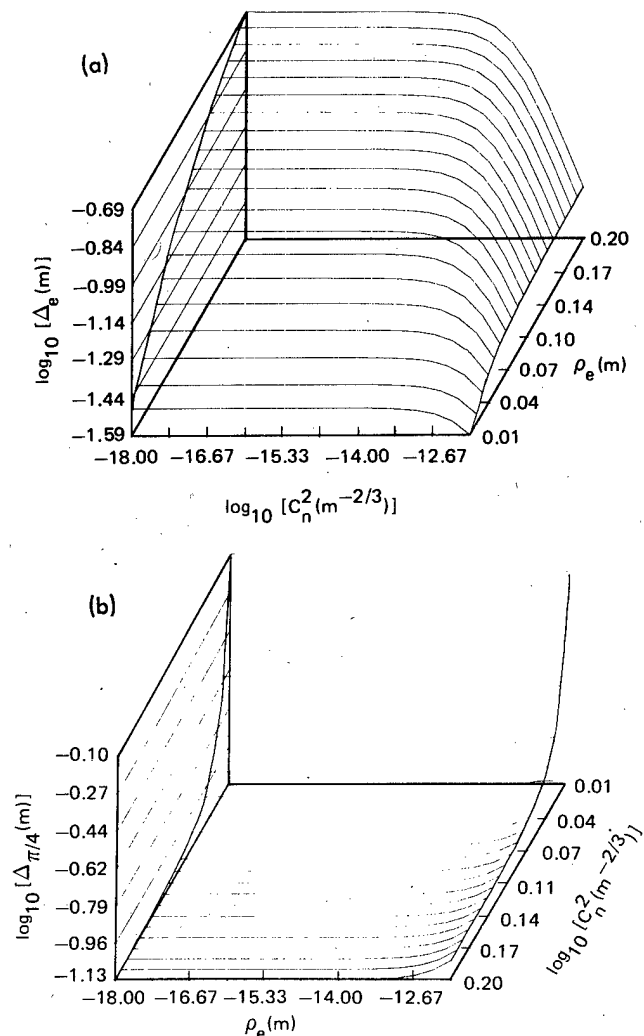


FIG. 5. Calculated values of the amplitude (a) and phase (b) coherence lengths as functions of the refractive-index structure constant (C_n^2) and source coherence length (ρ_e). Fixed parameters are $\lambda = 10^{-5}$ m, $L = 10^{-1}$ m, $R^+ = 10^3$ m, and $\theta^+ = 0^\circ$ [Fig. 5(a)] and $\theta^+ = 10^{-3}$ rad [Fig. 5(b)].

decrease of the predicted phase coherence length with increasing source coherence is again illustrated in Fig. 5(b), and it is additionally noted that the strength-of-turbulence affects this functional dependence appreciably only for the highest refractive-index structure constants (where the atmospheric coherence length becomes comparable to the source coherence length). Significantly, the amplitude coherence length increases rapidly for the high range of source coherence lengths plotted in Fig. 5(a), whereas the turbulence strength influences this functional dependence at the high values of the refractive-index structure constant.

A final illustration of the functional dependence of the field coherence predicted by the above analysis is provided by the Fig. 6 plots of the amplitude and phase coherence lengths as functions of the source size (L) and refractive-index structure constant. Both phase and amplitude coherence lengths display a similar functional form with respect to the variables plotted in Fig. 6. Clearly, the amplitude coherence lengths become speckle dominated for weak turbulence ($C_n^2 < 10^{-6}$) as evidenced by the constant, asymptotic relationship with respect to the strength-of-turbulence variable (C_n^2). Simi-

larly, the phase coherence length is constant for weak turbulence. However, in each case, atmospheric effects reduce the respective coherence lengths at high refractive-index structure-constant values with the onset of the reduction occurring earlier for the smaller source dimensions. The data plotted in Fig. 6 display trends similar to the predictions of Lee *et al.*⁷ for an incoherent source in the axial direction (Figs. 3-5 of Ref. 7).

REMARKS AND CONCLUSIONS

The theoretical foundation, provided above, has several significant advantages over previous investigations of turbulence effects on radiation propagation. The principal contributions of this analysis are (i) it is mathematically straightforward, (ii) it provides for the characterization of radiation derived from partially coherent sources throughout the full range of propagation directions, (iii) it includes the known features of (a) coherent radiation propagation in turbulence and (b) partially coherent radiation propagation *in vacuo*, and (iv) it permits a physical characterization of the

radiation coherence propagation in terms of scattering functions. Although the five-thirds law structure function was approximated by a quadratic function to permit explicit calculations of coherence effects, calculated plane-wave results are in sufficient agreement with experimental data to permit confidence in the general trends and magnitudes of coherence effects predicted by this approximation. Significantly, all of the predicted coherence effects derived from this approximation are consistent with physical intuition and approach proper limiting results over an appropriate range of propagation angle, source size, source coherence length, and turbulence strength variables. Although the definition of an effective far-field range for Gaussian partially coherent sources resulted from considerations unrelated to turbulence effects, this definition is significant because it extends the concept of the far field to partially coherent sources. While this extension is limited to partially coherent sources with Gaussian MCF's, it is likely that similar results obtain for other source MCF's because of the Fourier transform relationship [Eq. (20)] between the field-point MCF and the generalized source coherence.

The above analysis of the atmospheric propagation of partially coherent radiation should find application in areas where laser-illuminated objects viewed through the atmosphere are of interest (e.g., laser radars). Analyses have been developed (e.g., Refs. 25 and 26) for predicting the mutual coherence and intensity distribution of laser-illuminated rough surfaces. Because the foregoing development permits analysis of atmospheric modifications of vacuum distributions [via the convolution Eqs. (24) and (32)], theoretical investigations of turbulence effects on realistic laser-illuminated rough surfaces should be possible.

ACKNOWLEDGMENT

The assistance of J. M. Putnam, who developed the program to compute the three-dimensional graphs, is gratefully acknowledged.

APPENDIX A

Phase factor evaluation

The phase factor defined in Eq. (6) can be written

$$\begin{aligned} L(\mathbf{r}^+, \mathbf{r}^-, \mathbf{P}^+, \mathbf{P}^-) &= |\mathbf{r}^+ + \frac{1}{2}\mathbf{r}^- - \mathbf{P}^+ - \frac{1}{2}\mathbf{P}^-| - |\mathbf{r}^+ - \frac{1}{2}\mathbf{r}^- \\ &\quad - \mathbf{P}^+ + \frac{1}{2}\mathbf{P}^-| = [|\mathbf{r}^+ - \mathbf{P}^+|^2 + (\mathbf{r}^+ - \mathbf{P}^+) \cdot (\mathbf{r}^- - \mathbf{P}^-) \\ &\quad + \frac{1}{4}|\mathbf{r}^- - \mathbf{P}^-|^2]^{1/2} - [|\mathbf{r}^+ - \mathbf{P}^+|^2 - (\mathbf{r}^+ - \mathbf{P}^+) \cdot (\mathbf{r}^- - \mathbf{P}^-) \\ &\quad + \frac{1}{4}|\mathbf{r}^- - \mathbf{P}^-|^2]^{1/2} = |\mathbf{r}^+ - \mathbf{P}^+| \{1 + \frac{1}{2}[(\mathbf{r}^+ - \mathbf{P}^+) \cdot (\mathbf{r}^- - \mathbf{P}^-) \\ &\quad + \frac{1}{4}|\mathbf{r}^- - \mathbf{P}^-|^2] |\mathbf{r}^+ - \mathbf{P}^+|^{-2} + 0(|\mathbf{r}^+ - \mathbf{P}^+|^{-2}) - 1 \\ &\quad - \frac{1}{2}[-(\mathbf{r}^+ - \mathbf{P}^+) \cdot (\mathbf{r}^- - \mathbf{P}^-) + \frac{1}{4}|\mathbf{r}^- - \mathbf{P}^-|^2] |\mathbf{r}^+ - \mathbf{P}^+|^{-2} \\ &\quad - 0(|\mathbf{r}^+ - \mathbf{P}^+|^{-2})\} \approx (\mathbf{r}^- - \mathbf{P}^-) \cdot \hat{w}(\mathbf{r}^+, \mathbf{P}^+), \quad (\text{A1}) \end{aligned}$$

where

$$\begin{aligned} \hat{w}(\mathbf{r}^+, \mathbf{P}^+) &\equiv (\mathbf{r}^- - \mathbf{P}^-) / |\mathbf{r}^- - \mathbf{P}^-| \\ &= (\mathbf{r}^+ - R\hat{s}^+) (R^+)^{-1} [1 + (\mathbf{r}^+)^2 (R^+)^{-2} \\ &\quad - 2(\mathbf{r}^+ \cdot \hat{s}^+) (R^+)^{-2}]^{-1/2} \quad (\text{A2}) \end{aligned}$$

and the definitions of Eqs. (7)-(10) have been employed. The vector $w(\mathbf{r}^+, \mathbf{P}^+)$ is illustrated in Fig. 1. Because R^+ is much greater than a source dimension (by assumption),

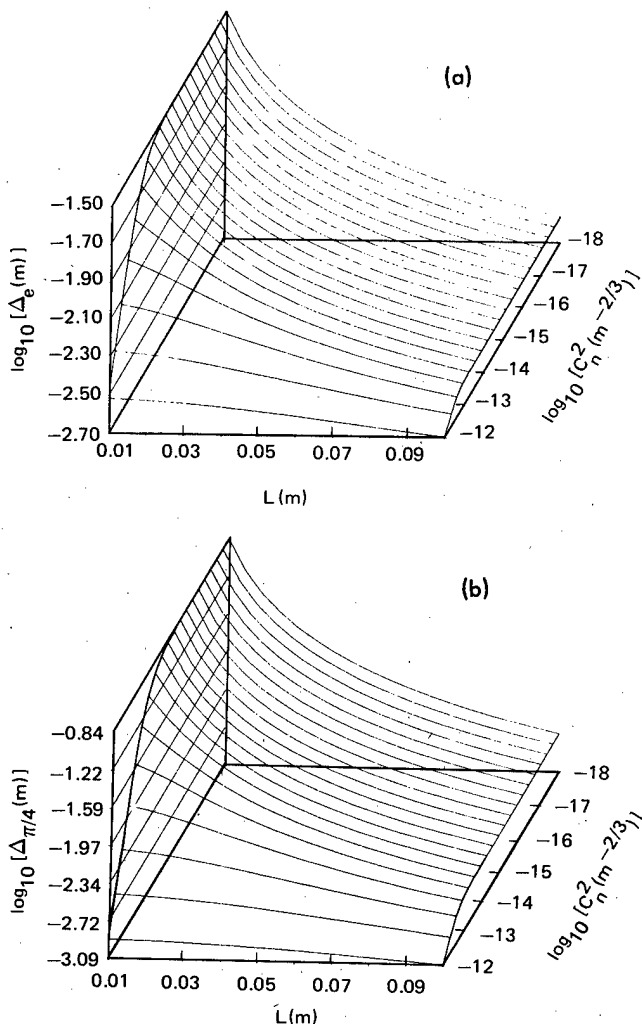


FIG. 6. Calculated values of the amplitude (a) and phase (b) coherence lengths as functions of the source size (L) and refractive-index structure constant (C_n^2). Fixed parameters are $\lambda = 10^{-6}$ m, $\rho_0 = 10^{-4}$ m, $R^+ = 10^3$ m, and $\theta^+ = 5^\circ$.

$$\dot{\omega}(\mathbf{r}^+, \mathbf{P}^+) \cong (\mathbf{r}^+/R^+ - \hat{s}^+). \quad (\text{A3})$$

Using Eq. (A3) and the fact that

$$\mathbf{P}^- = R^+\hat{s}^- + R^-\hat{s}^+, \quad (\text{A4})$$

together with the knowledge that \hat{s}^+ and \hat{s}^- are orthogonal vectors (\hat{s}^+ is a unit vector), Eq. (A1) can be written

$$L(\mathbf{r}^+, \mathbf{r}^-, \mathbf{P}^+, \mathbf{P}^-) = [\mathbf{r}^- \cdot \mathbf{r}^+/R^+ - \mathbf{r}^- \cdot \hat{s}^+ - \mathbf{r}^+ \cdot \hat{s}^- + R^-(1 - \hat{s}^+ \cdot \mathbf{r}^+/R^+)]. \quad (\text{A5})$$

However, again noting the small value of (\mathbf{r}^+/R^+) over the range of integration considered, Eq. (A5) becomes

$$L(\mathbf{r}^+, \mathbf{r}^-, \mathbf{P}^+, \mathbf{P}^-) \cong [\mathbf{r}^- \cdot \mathbf{r}^+/R^+ - \mathbf{r}^- \cdot \hat{s}^+ - \mathbf{r}^+ \cdot \hat{s}^- + R^-] \quad (\text{A6})$$

to an excellent approximation.

APPENDIX B

Uniform coherent source MCF and spectral density evaluation

A uniform coherent source is characterized by a source MCF of the form

$$\Gamma_s(\mathbf{r}^+, \mathbf{r}^-) = |U_0|^2. \quad (\text{B1})$$

Therefore, the generalized two field-point source coherence [Eq. (15)] is given by

$$G = (2\pi)^2(R^+/k)^2 A^{-1} |U_0|^2 \delta(\mathbf{r}^- - R^+\hat{s}^-), \quad (\text{B2})$$

and hence the predicted MCF is [Eq. (17)],

$$\Gamma^{\text{turb}}(\mathbf{P}^+, \mathbf{P}^-) = |U_0|^2 \cos^2\theta^+$$

$$\begin{aligned} & \times \int \int_{-\infty}^{\infty} d^2\mathbf{r}^- e^{-i(k\mathbf{r}^-) \cdot \hat{s}^+} \delta(\mathbf{r}^- - R^+\hat{s}^-) F(\mathbf{r}^-, \mathbf{P}^-) \\ & = |U_0|^2 \cos^2\theta^+ e^{ikR^+\hat{s}^- \cdot \hat{s}^+} F(R^+\hat{s}^-, \mathbf{P}^-) \\ & = |U_0|^2 \cos^2\theta^+ F(\mathbf{P}^-, \mathbf{P}^-), \end{aligned} \quad (\text{B3})$$

assuming equidistant radial field-point separations (i.e., $R^- = 0$). Equation (38) can be easily integrated using the conditions of equal source-point and field-point separations imposed by Eq. (B3); the result is

$$F(\mathbf{P}^-, \mathbf{P}^-) = \exp[-3(\rho/\rho_0)^2], \quad (\text{B4})$$

where

$$\rho = |\mathcal{P}(\mathbf{P}^-)|.$$

Equations (B3) and (B4) express the plane-wave MCF result using the quadratic approximation [Eq. (38)]. Note that the coherence length predicted by this approximation is

$$\rho(e^{-1})|_{\text{plane-wave}} = (1/\sqrt{3})\rho_0 = 0.58\rho_0, \quad (\text{B5})$$

which is in good agreement with the value of $0.56\rho_0$ predicted by the five-thirds law.

Artem'ev and Gurvich²¹ have performed optical measurements of the spectral density of field fluctuations using the Fourier-transform properties of a simple lens. Accordingly, their dimensionless spectral density results are defined in the following terms:

$$V(\bar{\chi}) = J(\bar{\chi})/J(0), \quad (\text{B6})$$

where

$$J(y) = \int_0^\infty \Gamma^{\text{turb}}(R^+, 2R_0t) \cos[(2kR_0y/F_0)t] dt, \quad (\text{B7})$$

$$\bar{\chi} = 2kR_0yF_0^{-1}[D_1(2R_0)]^{-3/5}, \quad (\text{B8})$$

F_0 is lens focal length, $2R_0$ is lens diameter, and D_1 is the complex phase structure function for the assumed plane wave. Fourier transforming the plane-wave MCF predicted by Eqs. (B3) and (B4) according to the prescription of Eq. (B7) yields the following result:

$$V(\bar{\chi}') = \exp[-(1/48)\bar{\chi}'^2 \rho_0^2 R_0^{-2} D_1(2R_0)], \quad (\text{B9})$$

where the dimensionless variable $\bar{\chi}$ has been redefined

$$\bar{\chi}' = 2kR_0yF_0^{-1}[D_1(2R_0)]^{-1/2} \quad (\text{B10})$$

in accord with the quadratic assumption. Because the plane-wave MCF result in the quadratic approximation implies a structure function defined by

$$\frac{1}{2}D_1(\rho) = 3(\rho/\rho_0)^2, \quad (\text{B11})$$

Eq. (B9) reduces to

$$V(\bar{\chi}) = \exp(-\bar{\chi}^2/2). \quad (\text{B12})$$

Equation (B12) is plotted in Fig. 2 together with experimental data of Artem'ev and Gurvich.²¹

APPENDIX C

Two-source spherical wave MCF evaluation

To perform the projection operations indicated in Eq. (38), orthogonal unit vectors \hat{a}_1 and \hat{a}_2 are constructed which define a plane transverse to the \mathbf{P}^+ direction. These vectors are

$$\begin{aligned} \hat{a}_1 &= [\hat{s}^+ \times \hat{k}][1 - (\hat{s}^+ \cdot \hat{k})^2]^{-1/2} \\ &= -\hat{i} \cos\phi - \hat{j} \sin\phi, \end{aligned} \quad (\text{C1})$$

$$\begin{aligned} \hat{a}_2 &= \hat{a}_1 \times \hat{s}^+ \\ &= -\hat{i} \cos\theta^+ \sin\phi + \hat{j} \cos\theta^+ \cos\phi + \sin\theta^+ \hat{k}. \end{aligned} \quad (\text{C2})$$

Therefore,

$$\begin{aligned} \mathcal{P}(\mathbf{r}^-) &= (\hat{a}_1 \cdot \mathbf{r}^-)\hat{a}_1 + (\hat{a}_2 \cdot \mathbf{r}^-)\hat{a}_2 \\ &= -\hat{a}_1(x^- \cos\phi + y^- \sin\phi) \\ &\quad + \hat{a}_2(-x^- \sin\phi + y^- \cos\phi) \cos\theta^+. \end{aligned} \quad (\text{C3})$$

The vector difference vector \hat{s}^- can be written

$$\hat{s}^- = \hat{s}^+ \times d\Omega, \quad (\text{C4})$$

where

$$\hat{s}^+ = \hat{i} \sin\phi \sin\theta^+ - \hat{j} \sin\theta^+ \cos\phi + \hat{k} \cos\theta^+, \quad (\text{C5})$$

and

$$d\Omega \cong \delta \cos\phi \hat{i} + \delta \sin\phi \hat{j} + \omega \hat{k} \quad (\text{C6})$$

is the axial vector corresponding to the antisymmetric rotation tensor that carries \hat{s}^+ into \hat{s}^- (in the small-angle approximation). Performing the vector multiplication of Eq. (C4) using the expressions (C5) and (C6) and performing the projection operation indicated in Eq. (C3) yields

$$\mathcal{P}(\mathbf{P}^-) = R^+(\omega \sin\theta \hat{a}_1 + \delta \hat{a}_2), \quad (\text{C7})$$

where

$$\mathbf{P}^- = R^+ \hat{s}^- + R^- \hat{s}^+ \quad (C8)$$

Because the problem is azimuthally symmetric, the plane included by the y axis is chosen (i.e., $\phi = \pi$) so that

$$|t\mathcal{P}(\mathbf{P}^-) + (1-t)\mathcal{P}(\mathbf{r}^-)|^2 = t^2[(R^+ \omega \sin\theta^+ - x^-)^2 + (R^+ \delta + y^- \cos\theta^+)^2] + 2t[x^-(R^+ \omega \sin\theta^+ - x^-) - y^- \cos\theta^+(R^+ \delta + y^- \cos\theta^+)] + [(x^-)^2 + (y^- \cos\theta^+)^2]. \quad (C9)$$

Employing the definitions of Eqs. (48) and (53) yields

$$F(\mathbf{r}^-, \mathbf{P}^-, R^+) = \exp\{- (R/\rho_0)^2 [(b + \beta)^2 + (c - \delta)^2 + c\delta - b\beta]\} \quad (C10)$$

upon integrating Eqs. (38) using Eq. (C9).

Utilizing the definition of the pseudo-scattering function [Eq. (22)] together with the above result for the two-source spherical-wave MCF yields

$$\begin{aligned} \hat{F}(\hat{\xi}; \hat{s}^-, R^+) &= (kR^+)^2 \sec\theta^+ \exp\left[-\frac{3}{4}\left(\frac{R^+}{\rho_0}\right)^2 (\beta^2 + \delta^2)\right] \\ &\times \int_{-\infty}^{\infty} db \int_{-\infty}^{\infty} dc \exp\left\{-\left(\frac{R^+}{\rho_0}\right)^2 \left[\left(b + \frac{\beta}{2}\right)^2 + \left(c - \frac{\delta}{2}\right)^2\right]\right\} \\ &\times \exp[-i(kR^+)(\xi_x b + \sec\theta^+ \xi_y c)] \\ &= \pi(k\rho_0)^2 \sec\theta^+ \exp\left[-\frac{3}{4}\left(\frac{R^+}{\rho_0}\right)^2 (\beta^2 + \delta^2)\right] \\ &\times \exp\left(-\frac{1}{4}(k\rho_0)^2 (\xi_x^2 + \xi_y^2 \sec^2\theta^+)\right) \\ &\times \exp\left[i\left(\frac{kR^+}{2}\right) (\xi_x \beta - \xi_y \delta \sec\theta^+)\right] \quad (C11) \end{aligned}$$

after changing variables and integrating.

*This research was conducted under the McDonnell Douglas Independent Research and Development program.

¹M. J. Beran, "Propagations of a finite beam in a random medium," *J. Opt. Soc. Am.* **60**, 518-521 (1970).

²R. L. Fante, "Mutual coherence function and frequency spectrum of a laser beam propagating through atmospheric turbulence," *J. Opt. Soc. Am.* **64**, 592-598 (1974).

³V. I. Tatarskii, "The effects of the turbulent atmosphere on wave propagation," translated from the Russian TT-68-50464, 472 pp., National Technical Information Service, U.S. Dept. of Commerce, Springfield, Va. 22151.

⁴W. P. Brown, "Second moment of a wave propagating in a random medium," *J. Opt. Soc. Am.* **61**, 1051-1059 (1971).

⁵H. T. Yura, "Mutual coherence function of a finite cross section

optical beam propagating in a turbulent medium," *Appl. Opt.* **11**, 1399-1406 (1972).

⁶M. J. Beran, "Coherence equations governing propagation through random media," *Radio. Sci.* **10**, 15-21 (1975).

⁷M. H. Lee, J. F. Holmes, and J. R. Kerr, "Statistics of speckle propagation through the turbulent atmosphere," *J. Opt. Soc. Am.* **66**, 1164-1172 (1976).

⁸R. F. Lutomirski and H. T. Yura, "Propagation of a finite optical beam in an inhomogeneous medium," *Appl. Opt.* **10**, 1652-1658 (1971).

⁹E. Wolf and W. H. Carter, "Angular distribution of radiant intensity from sources of different degrees of spatial coherence," *Opt. Commun.* **13**, 205-209 (1975).

¹⁰R. L. Fante and J. L. Poirier, "Mutual coherence function of a finite optical beam in a turbulent medium," *Appl. Opt.* **12**, 2247-2248 (1973).

¹¹E. W. Marchand and E. Wolf, "Angular correlation and the far-zone behavior of partially coherent fields," *J. Opt. Soc. Am.* **62**, 379-385 (1972).

¹²The vector problem can be treated using the technique described in this paper together with the formalism described in J. C. Leader, "The generalized partial coherence of a radiation source and its far-field" *Optica Acta* (to be published).

¹³A. Sommerfeld, "Optics," *Lectures on Theoretical Physics* (Academic, New York, 1954), Vol IV, pp. 197-201.

¹⁴R. K. Luneburg, *Mathematical Theory of Optics* (University of California, Berkeley, 1964), pp. 311-319.

¹⁵M. Born and E. Wolf, *Principles of Optics*, 3rd (revised) edition (Pergamon, New York, 1965), pp. 512-513.

¹⁶Use has been made of the fact that $R^- = (|\mathbf{p}|^2 + z^2)^{1/2} - (|\mathbf{p}'|^2 + z^2)^{1/2} \approx (1/2z)$

$$\times (|\mathbf{p}|^2 - |\mathbf{p}'|^2) = \mathbf{p}^+ \cdot \mathbf{p}^- / z.$$

¹⁷M. J. Beran and G. B. Parrent, *Theory of Partial Coherence* (Prentice-Hall, Englewood Cliffs, N.J., 1964), Eqs. 4-25.

¹⁸D. L. Fried, "Optical resolution through a randomly inhomogeneous medium for very long and very short exposures," *J. Opt. Soc. Am.* **56**, 1372-1384 (1966).

¹⁹A. Kon and V. Feizulin, "Fluctuations in the parameters of spherical waves propagating in a turbulent atmosphere," *Radiophys. Quantum Electron. (USSR)* **13**, 51-53 (1970).

²⁰R. L. Fante, "Two-source spherical wave structure functions in atmospheric turbulence," *J. Opt. Soc. Am.* **66**, 74 (1976).

²¹A. V. Artem'ev and A. S. Gurvich, "Experimental study of coherence function spectra," *Radiophys. Quantum Electron. (USSR)* **14**, 580-583 (1971).

²²D. E. Barrick, "Rough surface scattering based on the specular point theory," *IEEE Trans. Antennas Propag.* **AP-16**, 449-454 (1968).

²³J. R. Dunphy and J. R. Kerr, "Turbulence effects on target illumination by laser sources: phenomenological analysis and experimental results," *Appl. Opt.* **16**, 1345-1358 (1977).

²⁴Ref 17, pp. 50-52.

²⁵J. C. Leader, "An analysis of the spatial coherence of laser light scattered from a surface with two scales of roughness," *J. Opt. Soc. Am.* **66**, 536-546 (1976).

²⁶J. C. Leader, "Incoherent backscatter from rough surfaces: the two scale model re-examined," *Radio. Sci.* (to be published June/July 1978).